The intersection graph of the disks with diameters the sides of a convex n-gon[*]

Clemens Huemer[†] Pablo Pérez-Lantero[‡]

September 2, 2019

Abstract

Given a convex polygon of n sides, one can draw n disks (called side disks) where each disk has a different side of the polygon as diameter and the midpoint of the side as its center. The intersection graph of such disks is the undirected graph with vertices the n disks and two disks are adjacent if and only if they have a point in common. We introduce the study of this graph by proving that it is planar for every convex polygon.

Keywords: Intersection Graph, Planarity, Disks, Convex Polygon.
MSC: 05C10, 52C99.

1 Introduction

Let P_n be a convex polygon of n sides denoted $s_0, s_1, \dots, s_{n-1}$ counter-clockwise. For each side s_i, let D_i denote the disk with diameter the length of s_i and center the midpoint of s_i. Since D_i is constructed on the side s_i of P_n, we say that D_i is a *side disk* of P_n. The *intersection graph* of the side disks $D_0, D_1, \dots, D_{n-1}$ is the undirected graph $G = (V, E)$, where $V = \{D_0, D_1, \dots, D_{n-1}\}$ and $\{D_i, D_j\} \in E$ if and only if the intersection of D_i and D_j is not empty. In this paper, we prove that for any convex polygon the intersection graph of the side disks is planar, introducing the study of this new class of geometric intersection graphs.

Geometric intersection graphs are a research topic in combinatorics and discrete and computational geometry (see for instance [1]). Furthermore, results on disjoint and/or intersecting disks in the plane are among the most classical ones in discrete geometry. For example, a theorem of Danzer [3] says that if any two of a given family of n disks intersect, then there exists a set of four points which intersects each disk. Intersections of disks have also been considered in the context of intersection graphs: each disk represents a vertex of the graph and two vertices are adjacent if

[*]The partial solution for the convex pentagon appeared at the XVI Spanish Meeting on Computational Geometry, Barcelona, Spain, 2015 [8].

[†]Departament de Matemàtiques, Universitat Politècnica de Catalunya, Barcelona, Spain. `clemens.huemer@upc.edu`.

[‡]Departamento de Matemática y Ciencia de la Computación, Universidad de Santiago, Santiago, Chile. `pablo.perez.l@usach.cl`.

This work has received funding from the European Union's Horizon 2020 research and innovation programme under the Marie Skłodowska-Curie grant agreement No 734922.

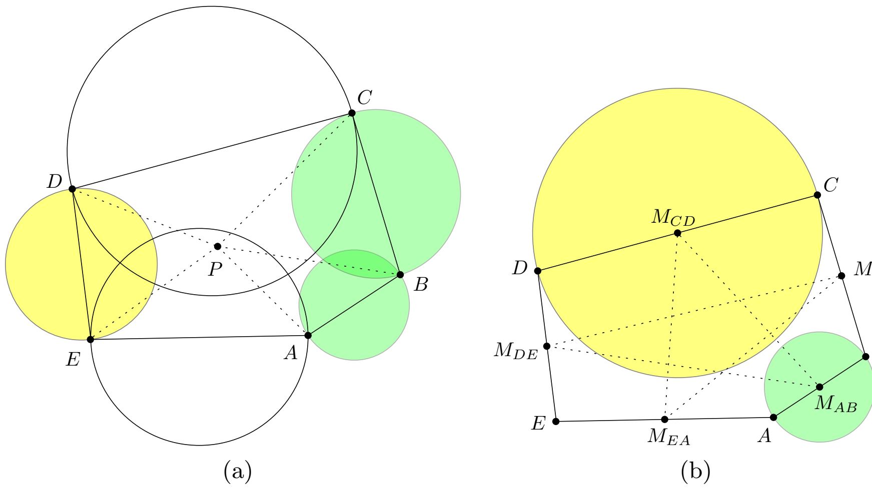

Figure 1: (a) P lies outside the disks with diameters AB, BC, and DE. (b) Two disjoint disks with diameters AB and CD.

and only if the corresponding disks intersect. By the Koebe-Andreev-Thurston theorem [10], every planar graph is an intersection graph of disks, where every pair of intersecting disks have only one point in common, that is, they are tangent. In this paper, the disks are in special position and we prove that their intersection graph is planar.

The problem studied here, specifically the case of a pentagon, has been motivated from an attempt to improve the known lower and upper bounds on the minimum number of triples of points defining an obtuse angle, in a finite point set in the plane. Refer to the works of Conway et al. [2] and Fabila-Monroy et al. [4] for this combinatorial problem. This apparent easy case of a pentagon, where one has to show that two of the five side disks are disjoint, received the attention of several researchers of the discrete and computational geometry community, and turned out to be non-trivial to solve [8]. A quite natural approach is to connect an interior point P of the pentagon with the five vertices and consider the angles at P. It follows from Thales' Theorem that P lies in the disk with, say, diameter AE if and only if the angle $\angle APE$ is non-acute (i.e., $\angle APE \geq \pi/2$), and this reflects the relation with the above mentioned combinatorial problem. In Figure 1a, P lies outside the disks with diameters AB, BC, and DE. Clearly, no point P lies in more than three of the five disks, since otherwise the five angles around P would sum more than 2π. One could then use a fractional version of Helly's theorem (Theorem 12 in [14]), which states that if among all the 10 triples of the five disks, more than 6 triples have a point in common, then there exists a point contained in 4 disks. We conclude that there are at least 4 triples of disks without a common intersection. However, it remained elusive to us to solve this particular case with a Helly-type approach. Another tentative approach that fails is the following: Let us consider the example in Figure 1b. The two side disks corresponding to sides AB and CD are disjoint. This is equivalent to saying that the distance between the midpoints M_{AB} and M_{CD} of the segments AB and CD, respectively, is larger than the sum of the radii of the disks, equal to half of the sum of the lengths of AB and CD. Thus, a natural approach is to prove that the sum of the five distances between the midpoints (that is, the dotted edges in Figure 1b) is bigger than the perimeter of the pentagon. But this is not always the case: for example, consider the pentagon with vertices at $(1, 9)$, $(0, 3)$, $(0, -3)$, $(1, -9)$, and $(60, 0)$.

Further notation: Given three different points p, q, and r in the plane, let $\ell(p,q)$ denote the straight line containing both p and q, $pq \subset \ell(p,q)$ the segment with endpoints p and q, $h(p,q)$ the halfline emanating from p and containing q, Δpqr the triangle with vertex set $\{p,q,r\}$, and $\angle pqr$ the angle not bigger than π with vertex q and sides $h(q,p)$ and $h(q,r)$. For a line ℓ, let $dist(p,\ell)$ denote the distance from p to ℓ. Given a segment s, let $|s|$ denote the length of s, $\ell(s)$ the line that contains s, and D_s the disk that has diameter $|s|$ and center the midpoint of s. We say that a (convex) quadrilateral is *tangential* if each of its sides is tangent to the same given disk contained in the quadrilateral. Every time we define a polygon by enumerating its vertices, the vertices are given in counter-clockwise order. We will also refer to a polygon by giving a sequence of its vertices in counter-clockwise order.

2 Preliminaries

Let $s_0, s_1, \ldots, s_{n-1}$ denote in counter-clockwise order the sides of a convex polygon P_n. Let $D_0, D_1, \ldots, D_{n-1}$ be the side disks of P_n at $s_0, s_1, \ldots, s_{n-1}$, respectively, and $G = (V, E)$ the intersection graph of $D_0, D_1, \ldots, D_{n-1}$. Note that $\{D_i, D_{i+1}\} \in E$ for every $i \in \{0, 1, \ldots, n-1\}$, where subindices are taken modulo n. Then, G is Hamiltonian, with cycle $(D_0, D_1, \ldots, D_{n-1}, D_0)$.

Every Hamiltonian graph $G = (V, E)$ with a Hamiltonian cycle $c = (v_0, v_1, \ldots, v_{n-1}, v_0)$ can be embedded in the plane as follows: $v_0, v_1, \ldots, v_{n-1}$ are different points of the unit circle so that the edges of the cycle are the circular arcs between consecutive points, and any other edge $\{v_i, v_j\} \in E$ is the straight chord of the circle, denoted $\mathsf{c}_{i,j}$, that connects the points representing v_i and v_j, respectively. We call such an embedding as the *circular embedding* of G, using c. The chords induce the intersection graph $G_\mathsf{c} = (V_\mathsf{c}, E_\mathsf{c})$ (known as *circle graph*), where V_c is the set of chords, and $\{\mathsf{c}_{i,j}, \mathsf{c}_{k,\ell}\} \in E_\mathsf{c}$ if and only if the chords $\mathsf{c}_{i,j}$ and $\mathsf{c}_{k,\ell}$ have an interior point in common. Observe that subindices i, j, k, and ℓ must be different. See Figure 2 for examples.

Kuratowski [11] and Wagner [13] theorems are well-known characterizations of planar graphs, but they are oriented to general graphs. On the other hand, in most of the cases when proving that a graph is planar, one tries to find a way of drawing (i.e., embedding) the graph in the plane without crossings between the edges. In our particular case, we consider the condition that the intersection graph of the side disks of a convex polygon is always Hamiltonian, and use a particular characterization. Let $G = (V, E)$ be a Hamiltonian graph of n vertices, and let $c = (v_0, v_1, \ldots, v_{n-1}, v_0)$ be a Hamiltonian cycle of G. Assume that G is also planar. Note that any planar embedding $planar(G)$ of G satisfies the next conditions: The cycle c is a Jordan curve, $v_0, v_1, \ldots, v_{n-1}$ are consecutive points along c, and every edge $\{v_i, v_j\} \in E$ not in c (i.e., $j \neq i+1$) is a curve connecting points v_i and v_j through either c_{in} or c_{out}, where c_{in} and c_{out} are the interior and exterior regions of the plane defined by c, respectively. Color every edge through c_{in} in red, and every edge through c_{out} in blue. Consider now the circular embedding $circ(G)$ of G, using c. If we map $planar(G)$ to $circ(G)$, then every chord of $circ(G)$ is colored red or blue, and only chords of different colors can have an interior point in common. This shows that the chord intersection graph G_c is bipartite. Furthermore, the following characterization holds:

Theorem 1 ([9])**.** *Let $G = (V, E)$ be a Hamiltonian graph, and $G_\mathsf{c} = (V_\mathsf{c}, E_\mathsf{c})$ the intersection graph of the chords in a circular embedding of G. Then, G is planar if and only if G_c is bipartite.*

Any convex n-gon is the intersection of n halfplanes, where the boundary of each halfplane contains a side of the n-gon. In general, the intersection of n halfplanes is not always a convex

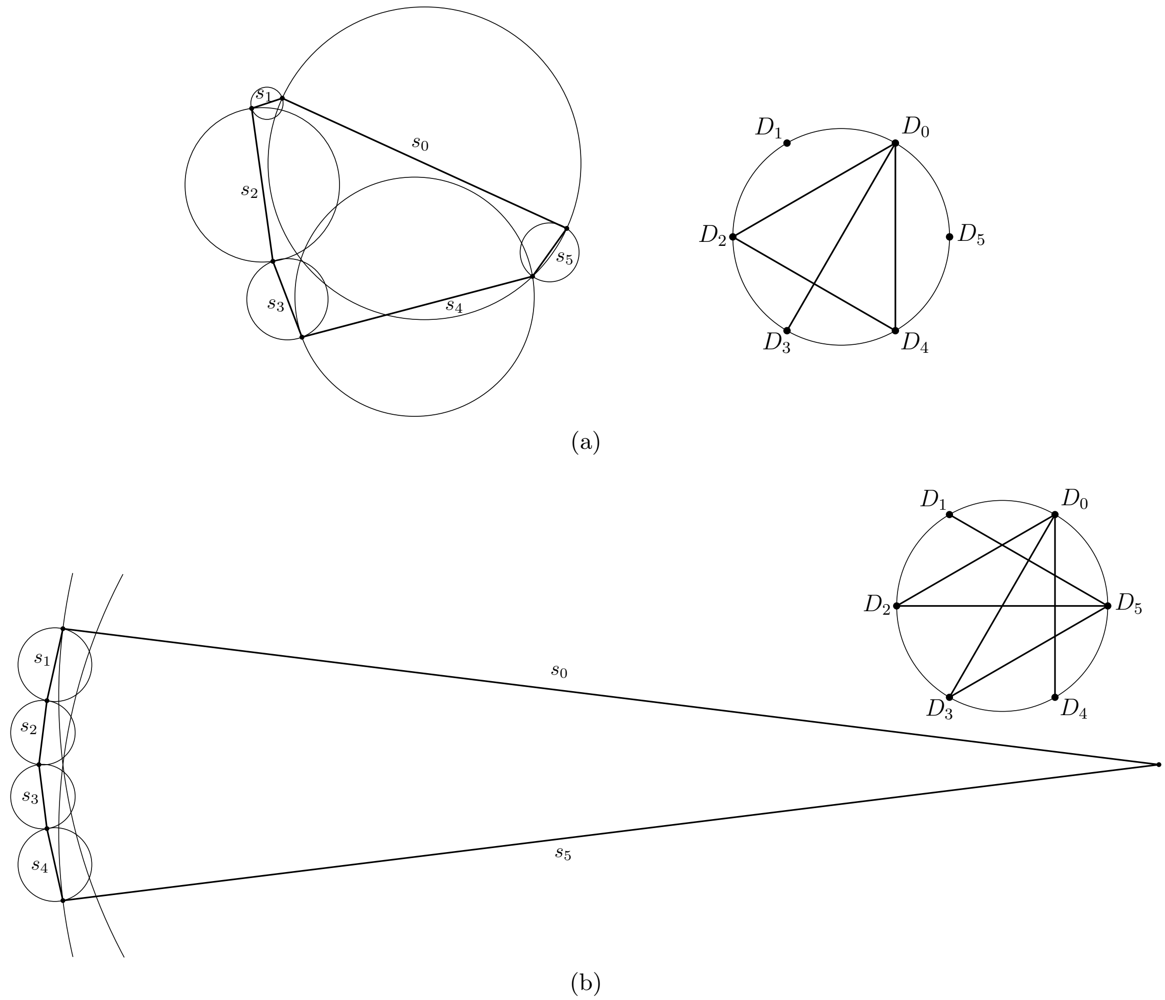

Figure 2: Two examples of an hexagon withs sides $s_0, s_1, \ldots, s_5$, together with the circular embedding of the intersection graph of the side disks.

polygon: it can be a convex unbounded set whose boundary is a connected polyline with the first and last sides being halflines instead of segments. We say that such a convex set is an *unbounded* convex n-gon, and if $s_0, s_1, \ldots, s_{n-1}$ denote the sides in counter-clockwise order, then s_0 and s_{n-1} are the first and last sides, that is, s_0 and s_{n-1} are halflines and $s_1, \ldots, s_{n-2}$ are segments. We consider in the case of an unbouded convex n-gon that s_0 and s_{n-1} *are not* consecutive sides, and the side disks at them are halfplanes as degenerated disks. In our proof we use both convex n-gons and unbounded convex n-gons. Given two sides of an (unbounded) convex polygon, the *bisector* is the line that contains the points of the polygon that are equidistant from the two sides.

To prove that G_{c} is bipartite, we will show that it does not have cycles of odd length, and the main results that we obtain in this direction are the following ones:

Lemma 2 (1-Chord). *Let P_n be an (unbounded) convex n-gon, $n \geq 5$, with sides denoted $s_0, s_1, \ldots, s_{n-1}$ in counter-clockwise order. Let $D_0, D_1, \ldots, D_{n-1}$ be the side disks of P_n at $s_0, s_1, \ldots,$ s_{n-1}, respectively. Then, there exists a side s_i such that the disk D_i intersects at most one disk*

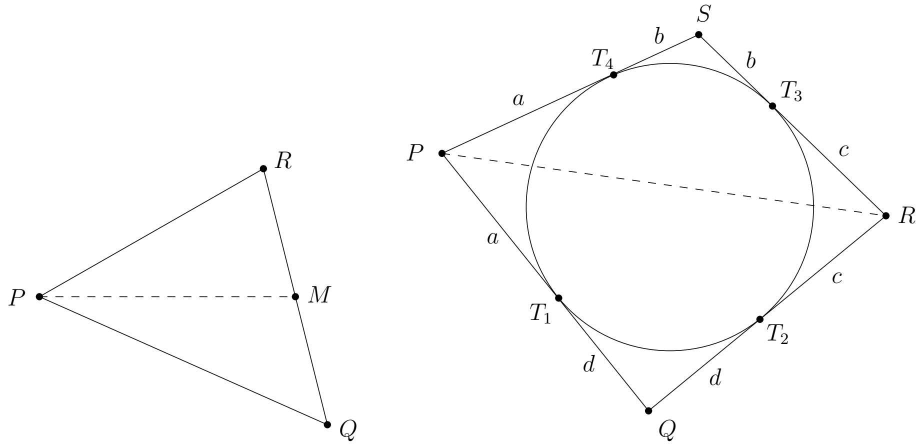

(a) (b)

Figure 3: (a) Illustration of Theorem 5. (b) Illustration of Lemma 6.

among the disks $D_{i+2}, D_{i+3}, \ldots, D_{i-3}, D_{i-2}$ not neighbouring D_i, where subindices are taken modulo n. That is, there is at most one chord with endpoint the point representing D_i in the circular embedding of the intersection graph of $D_0, D_1, \ldots, D_{n-1}$.

Lemma 3 (**No-3-Cycles**)**.** *Let P_n be an (unbounded) convex n-gon, $n \geq 6$, and* a, b, c, d, e, f *six sides appearing in this order counter-clockwise. At least one of the following statements is satisfied:*

(a) D_{a} and D_{d} are disjoint.

(b) D_{b} and D_{e} are disjoint.

(c) D_{c} and D_{f} are disjoint.

That is, the intersection graph of the chords in the circular embedding of the side disks of P_n does not have 3-length cycles.

Theorem 4 (**Main**)**.** *In any convex polygon, the intersection graph of the side disks is planar.*

We prove the above three results in sections 3, 4, and 5, respectively. In each section, we also prove several technical lemmas. The next basic results will be used:

Theorem 5 (Apollonius' Theorem)**.** *Let P, Q, and R be three different points of the plane, and let M denote the midpoint of the segment QR (see Figure 3a). Then, the length $|PM|$ satisfies:*

$$|PM| \ = \ \frac{1}{2}\sqrt{2\left(|PQ|^2 + |PR|^2\right) - |QR|^2}.$$

A known fact that we will also use is the following one: Given a disk and a point outside it, the two lines passing through the point and tangent to the disk define two segments of equal lengths. Each segment connects the point with a point of tangency between one of the lines and the disk.

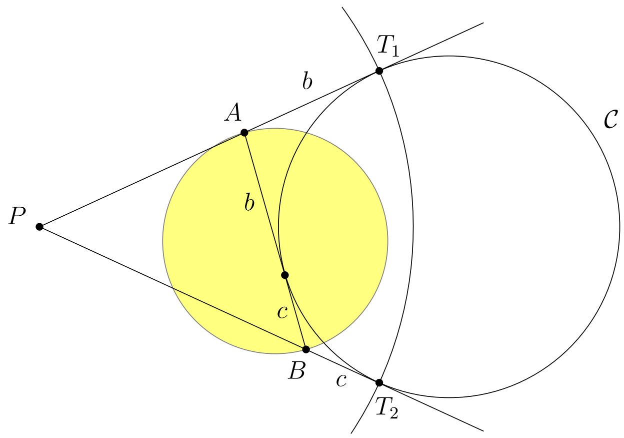

Figure 4: Illustration of Lemma 7.

Lemma 6 (Diagonal of a tangential quadrilateral [5])**.** *Let P, Q, R, and S be the vertices of a tangential quadrilateral, tangent to the disk $\mathcal{C}$. Let T_1, T_2, T_3, and T_4 denote the tangent points between the sides PQ, QR, RS, and SP and $\mathcal{C}$, respectively. Let $a = |PT_1| = |PT_4|$, $b = |ST_4| = |ST_3|$, $c = |RT_3| = |RT_2|$, and $d = |QT_2| = |QT_1|$ (see Figure 3b). Then, the length $|PR|$ satisfies:*

$$|PR| \;=\; \sqrt{\frac{a+c}{b+d} \cdot \big((a+c)(b+d)+4bd\big)}.$$

3 Part I: Proof of 1-Chord lemma (Lemma 2)

Lemma 7. *Let $\mathcal{C}$ be a disk and let P be a point not contained in $\mathcal{C}$. Let T_1 and T_2 be the points of the boundary of $\mathcal{C}$ such that the lines $\ell(P,T_1)$ and $\ell(P,T_2)$ are tangents to $\mathcal{C}$. Let A be a point in the segment PT_1 and B a point in the segment PT_2 such that the segment AB is tangent to $\mathcal{C}$ (see Figure 4). Then, the disk D_{AB} is contained in the disk with center P and radius $|PT_1| = |PT_2|$.*

Proof. Let $a = |PT_1| = |PT_2|$, $b = |AT_1|$, and $c = |BT_2|$. Let M denote the midpoint of the segment AB, and note that $|PA| = a - b$, $|PB| = a - c$, and $|AB| = b + c$. To prove the result, it suffices to prove that

$$|PM| + |MA| \;\leq\; a.$$

Note that $|PM| = (1/2)\sqrt{2((a-b)^2 + (a-c)^2) - (b+c)^2}$ by Theorem 5, and that $|MA| = (b+c)/2$. Since $b \leq a$ and $c \leq a$, which implies $(b+c)/2 \leq a$, verifying the above inequation is equivalent to proving that

$$4 \cdot |PM|^2 \;=\; 2((a-b)^2 + (a-c)^2) - (b+c)^2 \;\leq\; (2a - (b+c))^2 .$$

This last equation holds since the following inequalities are equivalent

$$\begin{aligned} 2((a-b)^2 + (a-c)^2) - (b+c)^2 &\leq (2a-(b+c))^2 \\ 4a^2 - 4ab - 4ac - 2bc + b^2 + c^2 &\leq 4a^2 + b^2 + c^2 - 4ab - 4ac + 2bc \\ 0 &\leq 4bc. \end{aligned}$$

The result thus follows. $\square$

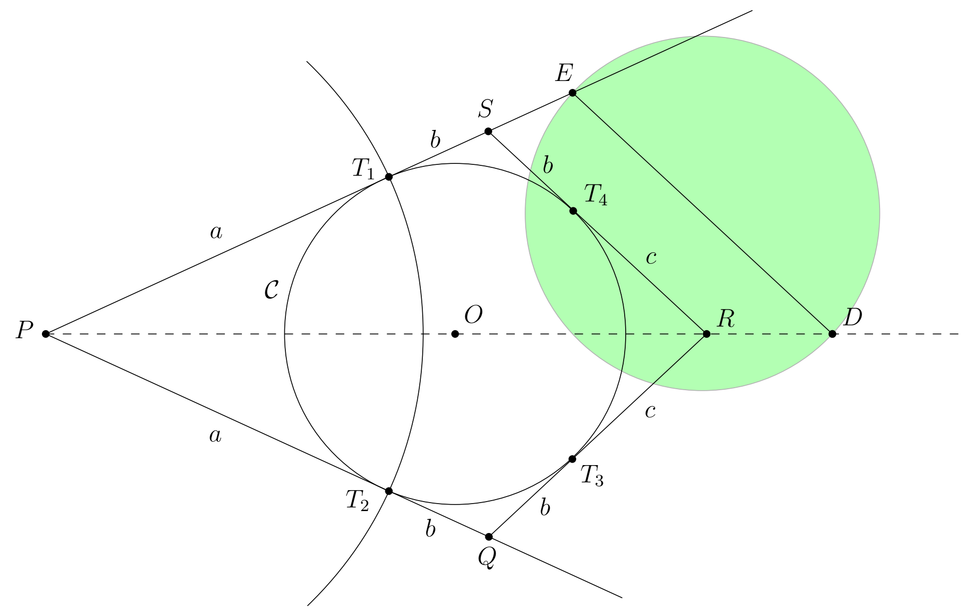

Figure 5: Illustration of Lemma 8.

Lemma 8. *Let $\mathcal{C}$ be a disk centered at the point O, and let P be a point not contained in $\mathcal{C}$. Let T_1 and T_2 be the points of the boundary of $\mathcal{C}$ such that the lines $\ell(P,T_1)$ and $\ell(P,T_2)$ are tangents to $\mathcal{C}$. Let E be a point in the halfline $h(P,T_1) \setminus PT_1$ and D a point in the halfline $h(P,O)$ such that: $\ell(E,D)$ does not intersect the interior of $\mathcal{C}$, and $\angle EDP \leq \pi/2$ (see Figure 5). Then, the disk D_{DE} does not intersect the disk with center P and radius $|PT_1| = |PT_2|$.*

Proof. Let $\mathcal{C}_P$ be the disk with center P and radius $|PT_1| = |PT_2|$. Let $S \in h(P,T_1) \setminus PT_1$ and $R \in h(P,O) \setminus PO$ be the points such that the line $\ell(S,R)$ is parallel to $\ell(E,D)$ and tangent to $\mathcal{C}$ at the point T_4. Let Q denote the reflection point of S about the line $\ell(P,O)$, and note that the quadrilateral with vertices P, Q, R, and S is a tangential quadrilateral, tangent to $\mathcal{C}$. Let T_3 be the point of tangency between the segment QR and $\mathcal{C}$, and $a = |PT_1| = |PT_2|$, $b = |ST_1| = |ST_4| = |QT_2| = |QT_3|$, and $c = |RT_3| = |RT_4|$. Then, by Lemma 6 used with $d = b$, we have that

$$|PR| \;=\; \sqrt{(a+c)(a+c+2b)}.$$

Let M denote the midpoint of the segment SR, which satisfies that $|MS| = (b+c)/2$. We claim that

$$|PT_1| + |MS| \;=\; a + (b+c)/2 \;<\; |PM|.$$

Indeed, by Theorem 5, we have that

$$\begin{aligned} |PM| &= \frac{1}{2}\sqrt{2\left(|PS|^2 + |PR|^2\right) - |SR|^2} \\ &= \frac{1}{2}\sqrt{2\left((a+b)^2 + (a+c)(a+c+2b)\right) - (b+c)^2}, \end{aligned}$$

and the inequalities

$$2a + b + c \;<\; 2 \cdot |PM|$$

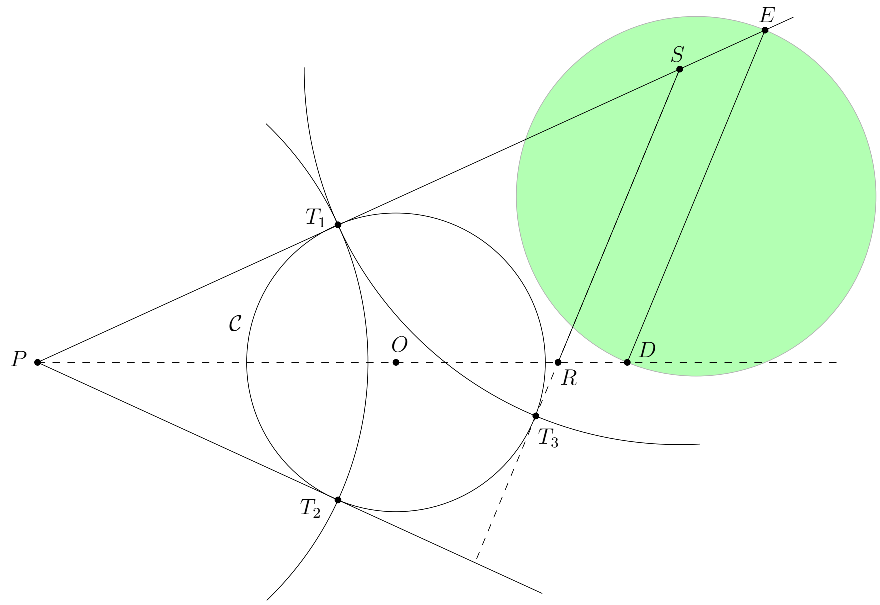

Figure 6: Illustration of Lemma 9.

$$\begin{aligned}
(2a+b+c)^2 &< 2\left((a+b)^2+(a+c)(a+c+2b)\right)-(b+c)^2 \\
4a^2+b^2+c^2+4ab+4ac+2bc &< 2(2a^2+b^2+c^2+4ab+2ac+2bc)-(b^2+c^2+2bc) \\
4a^2+b^2+c^2+4ab+4ac+2bc &< 4a^2+b^2+c^2+8ab+4ac+2bc \\
0 &< 4ab,
\end{aligned}$$

are all equivalent and hold given that $a,b>0$, which imply the claim. Let M' denote the midpoint of the segment ED. Since triangles ΔPRS and ΔPDE are similar, we have that $|PM'|=\lambda\cdot|PM|$ and $|M'E|=\lambda\cdot|MS|$, where $\lambda=|PE|/|PS|=|PD|/|PR|=|ED|/|SR|\geq 1$ is the similarity ratio between these triangles. Then, since $|PM|-|MS|>|PT_1|>0$, we have that

$$|PT_1| \;<\; |PM|-|MS| \;\leq\; \lambda(|PM|-|MS|) \;=\; |PM'|-|M'E|.$$

This immediately implies that the disk D_{DE} does not intersect the disk $\mathcal{C}_P$. $\square$

Lemma 9. *Let $\mathcal{C}$ be a disk centered at the point O, and let P be a point not contained in $\mathcal{C}$. Let T_1 and T_2 be the points of the boundary of $\mathcal{C}$ such that the lines $\ell(P,T_1)$ and $\ell(P,T_2)$ are tangents to $\mathcal{C}$. Let E be a point in the halfline $h(P,T_1)\setminus PT_1$ and D a point in halfline $h(P,O)$ such that: $\ell(E,D)$ does not intersect the interior of $\mathcal{C}$, and $\angle EDP>\pi/2$ (see Figure 7). Then, the disk D_{DE} does not intersect the disk $\mathcal{C}_P$ with center P and radius $|PT_1|=|PT_2|$.*

Proof. Let $S\in h(P,T_1)\setminus PT_1$ and $R\in h(P,O)\setminus PO$ be the points such that the line $\ell(S,R)$ is parallel to $\ell(E,D)$ and tangent to the disk $\mathcal{C}$ at the point T_3. Note that T_3 belongs to the wedge bounded by $h(P,O)$ and $h(P,T_2)$. Let $\mathcal{C}_S$ be the disk with center S and radius $|PT_1|=|PT_3|$ (see Figure 6). Since $\mathcal{C}_P$ and $\mathcal{C}_S$ have disjoint interiors and $D_{SR}\subset\mathcal{C}_S$, then $\mathcal{C}_P$ and D_{SR} are disjoint. Similar as in the last arguments of the proof of Lemma 8, D_{DE} does not intersect $\mathcal{C}_P$. $\square$

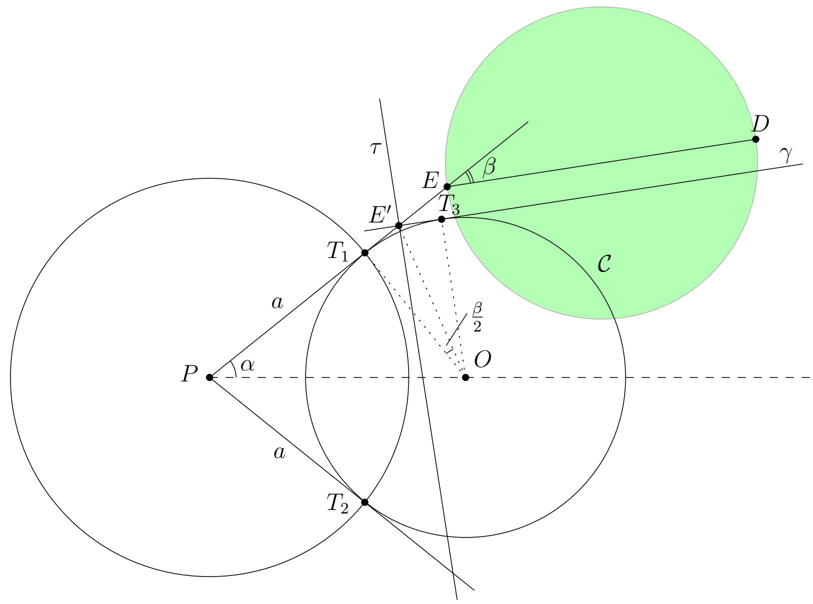

Figure 7: Illustration of Lemma 10.

Lemma 10. *Let $\mathcal{C}$ be a disk centered at the point O, and let P be a point not contained in $\mathcal{C}$. Let T_1 and T_2 be the points of the boundary of $\mathcal{C}$ such that the lines $\ell(P,T_1)$ and $\ell(P,T_2)$ are tangents to $\mathcal{C}$. Let E be a point in the halfline $h(P,T_1) \setminus PT_1$ and $D \neq E$ a point in the interior of the convex wedge bounded by $h(P,T_1)$ and $h(P,O)$ such that: $h(E,D)$ does not intersect with $h(P,O)$, and $\ell(E,D)$ does not intersect the interior of $\mathcal{C}$ (see Figure 7). Then, the disk D_{DE} does not intersect the disk with center P and radius $|PT_1| = |PT_2|$.*

Proof. Let $\alpha \in (0,\pi/2)$ denote the angle formed by $h(P,E)$ and $h(P,O)$, and $\beta \in (0,\alpha]$ the angle formed by $h(P,E)$ and $\ell(E,D)$ (see Figure 7). Let E' be the point in $h(P,T_1) \setminus PT_1$ such that the line different from $\ell(P,E')$ containing E' and tangent to $\mathcal{C}$, denoted γ, is parallel to the line $\ell(E,D)$. Let τ be the line perpendicular to γ that contains E', and T_3 denote the point of tangency between γ and $\mathcal{C}$. Let $a = |PT_1| = |PT_2|$, $b = |E'T_1| = |E'T_3|$, and r denote the radius of $\mathcal{C}$. Since the lines γ and τ are perpendicular, the angle formed by the lines $\ell(P,E')$ and τ is equal to $\pi/2-\beta$. Then, the distance $dist(P,\tau)$ from the point P to the line τ satisfies

$$dist(P,\tau) \;=\; |PE'| \cdot \sin(\pi/2-\beta) \;=\; (a+b)\cdot\cos\beta.$$

Note that $\angle T_1E'T_3 = \pi - \beta$. Then, since the line $\ell(O,E')$ bisects the angle $\angle T_1E'T_3$, we have that $\angle T_1E'O = \pi/2 - \beta/2$, which implies that

$$b = r\cdot\cot(\angle T_1E'O) = r\cdot\tan(\beta/2)$$

because the segment OT_1 satisfying $|OT_1| = r$ is perpendicular to the line $\ell(P,E')$. On the other hand, note that $a = r\cdot\cot\alpha$. Putting the above observations together, the next inequalities

$$\begin{aligned} |PT_1| &\leq dist(P,\tau) \\ a &\leq (a+b)\cdot\cos\beta \end{aligned}$$

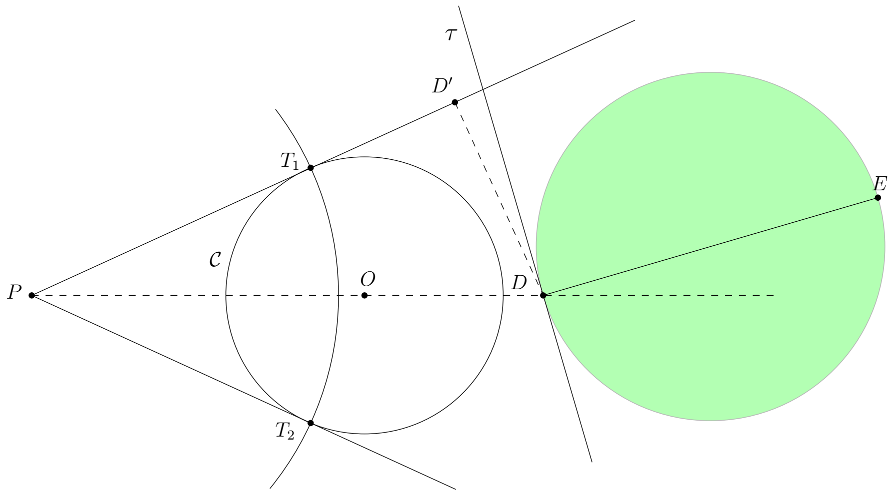

Figure 8: Illustration of Lemma 11.

$$
\begin{aligned}
r \cdot \cot\alpha &\leq (r \cdot \cot\alpha + r \cdot \tan(\beta/2)) \cdot \cos\beta \\
\cot\alpha &\leq \frac{\cos\beta \cdot \tan(\beta/2)}{1-\cos\beta} = \frac{\cos\beta \cdot \frac{\sin(\beta/2)}{\cos(\beta/2)}}{2\sin^2(\beta/2)} = \frac{\cos\beta}{2\sin(\beta/2)\cos(\beta/2)} \\
\frac{\cos\alpha}{\sin\alpha} &\leq \frac{\cos\beta}{\sin\beta} \\
0 &\leq \sin(\alpha-\beta)
\end{aligned}
$$

are all equivalent and hold given that $\beta > 0$ and $0 \leq \alpha - \beta < \alpha < \pi/2$. Since by construction the line τ either does not intersect the disk D_{DE} or is tangent to D_{DE} at the point $E' \neq T_1$, we can guarantee that the disk D_{DE} does not intersect the disk with center P and radius $|PT_1| = |PT_2|$. The lemma thus follows. $\square$

Lemma 11. *Let $\mathcal{C}$ be a disk centered at the point O, and let P be a point not contained in $\mathcal{C}$. Let T_1 and T_2 be the points of the boundary of $\mathcal{C}$ such that the lines $\ell(P,T_1)$ and $\ell(P,T_2)$ are tangents to $\mathcal{C}$. Let D be a point in the halfline $h(P,O) \setminus PO$ and E a point in the interior of the convex wedge bounded by $h(P,T_1)$ and $h(P,O)$ such that $h(D,E)$ does not intersect with $h(P,T_1)$ (see Figure 8). Then, the disk D_{DE} does not intersect the disk $\mathcal{C}_P$ with center P and radius $|PT_1| = |PT_2|$.*

Proof. Let τ be the line through D that is perpendicular to DE. Let D' be the orthogonal projection of D into $h(P,T_1)$, that is, lines $\ell(D,D')$ and $\ell(P,T_1)$ are perpendicular at D'. By the definition of E, the distante from P to τ is at least $|PD'|$ and at most $|PD|$. Since $|PT_1| < |PD|$, then the disks D_{DE} and $\mathcal{C}_P$ are disjoint. $\square$

Lemma 12. *Any (unbounded) convex n-gon, $n \geq 5$, contains a disk $\mathcal{C}$ tangent to three consecutive sides, such that: the lines containing the first and third sides, respectively, are not parallel and further their intersection point and the interior of $\mathcal{C}$ belong to different halfplanes bounded by the line containing the second side.*

Proof. Let P_n be a convex n-gon with sides denoted $s_0, s_1, \ldots, s_{n-1}$ counter-clockwise. In the following, every disk will be considered to be contained in P_n, and for every side s, let $\ell(s)$ denote

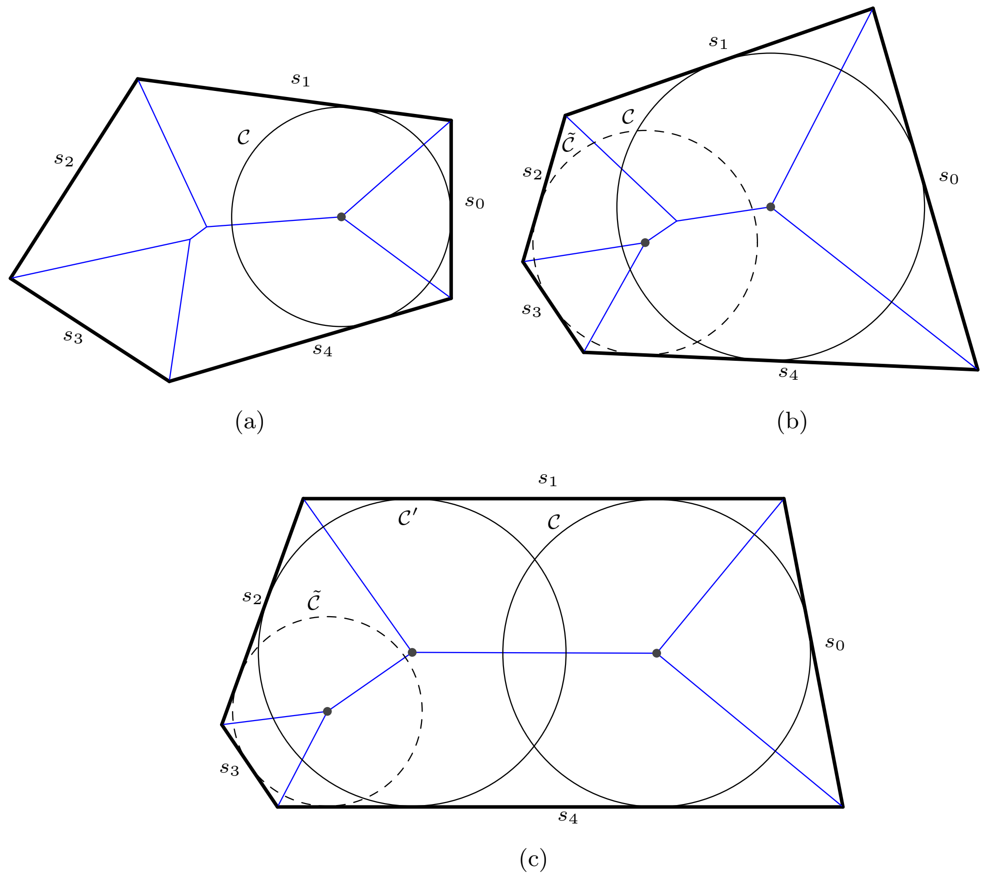

Figure 9: Proof of Lemma 12. (a) The medial axis of a convex pentagon with sides s_0, s_1, s_2, s_3, s_4, and a disk $\mathcal{C}$ tangent to the sides s_4, s_0, and s_1 and centered at a vertex of the medial axis. (b) If $\ell(s_4)$ and $\ell(s_1)$ are not parallel and their intersection point and the interior of $\mathcal{C}$ are at the same halfplane bounded by $\ell(s_0)$, and $\mathcal{C}$ is not tangent to both s_2 and s_3, then there exists a disk $\tilde{\mathcal{C}}$ with smaller radius tangent to three consecutive sides. (c) If $\ell(s_4)$ and $\ell(s_1)$ are parallel and $\mathcal{C}'$ is not tangent to s_3, then there exists a disk $\tilde{\mathcal{C}}$ with smaller radius tangent to three consecutive sides.

the line containing s. There exist disks tangent to three consecutive sides and centered at a vertex of the medial axis of P_n [12]. The medial axis of a simple polygon is the locus of the points of the polygon that have more than one closest point in the boundary. If the polygon is convex, the medial axis is a tree made of line segments, each contained in the bisector of two sides (see Figure 9a). Then, let $\mathcal{C}$ be a disk of minimum radius among those disks, tangent to the sides s_{n-1}, s_0, and s_1 w.l.o.g. If $\ell(s_{n-1})$ and $\ell(s_1)$ are not parallel and their intersection point and the interior of $\mathcal{C}$ are at different halfplanes bounded by $\ell(s_0)$ (see Figure 9a), then the lemma is proved. Otherwise, if $\ell(s_{n-1})$ and $\ell(s_1)$ are not parallel and their intersection point and the interior of $\mathcal{C}$ are at the same halfplane bounded by $\ell(s_0)$ (see Figure 9b), then by the minimality of $\mathcal{C}$ every side among $s_2, s_3, \ldots, s_{n-2}$ must be tangent to $\mathcal{C}$, which implies that every triple of consecutive sides among $s_1, s_2, \ldots, s_{n-1}$ together with $\mathcal{C}$ satisfy the conditions of the lemma. Finally, if $\ell(s_{n-1})$ and $\ell(s_1)$ are parallel (see Figure 9c), then by the minimality of $\mathcal{C}$ the disk $\mathcal{C}'$ with radius equal to that of $\mathcal{C}$ and tangent to the sides s_1 and s_{n-1}, and to at least one side s_i for some $i \in [2 \ldots n-2]$, must

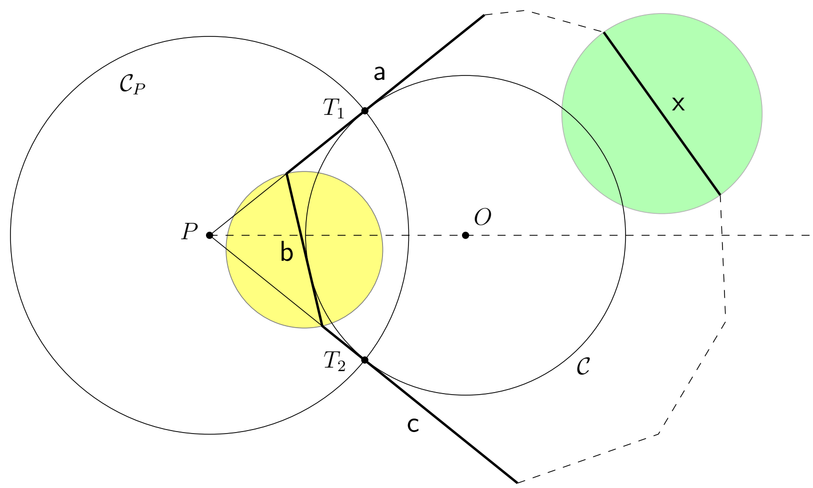

Figure 10: Proof of Lemma 13.

be tangent to all the sides $s_2, s_3, \ldots, s_{n-2}$. Since $n \geq 5$, every triple of consecutive sides among $s_1, s_2, \ldots, s_{n-1}$ and the disk $\mathcal{C}'$ prove the lemma. □

Lemma 13. *Let P_n be an (unbounded) convex n-gon, and* a, b, *and* c *three consecutive sides of P_n such that: the lines $\ell(\mathsf{a})$ and $\ell(\mathsf{c})$ intersect at point P, the line $\ell(\mathsf{b})$ separates the interior of P_n and P, and there exists a disk $\mathcal{C}$ with center O, contained in P_n, and tangent to* a, b, *and* c. *Then, for any side $\mathsf{x} \notin \{\mathsf{a}, \mathsf{b}, \mathsf{c}\}$ of P_n such that the bisector $\ell(P, O)$ of* a *and* c *does not intersect the interior of* x, *we have that D_{b} and D_{x} are disjoint (see Figure 10).*

Proof. Let T_1 and T_2 denote the points of tangency between $\mathcal{C}$ and the sides a and c, respectively, and $\mathcal{C}_P$ the disk with center P and radius $|PT_1| = |PT_2|$. Assume w.l.o.g. that x is contained in the convex wedge bounded by $h(P, T_1)$ and $h(P, O)$. By Lemma 7, we have that $D_{\mathsf{b}} \subset \mathcal{C}_P$. Furthermore, according to the relative position of x with respect to $h(P, T_1)$, $h(P, O)$, and $\mathcal{C}$, we can use Lemma 8, Lemma 9, Lemma 10, or Lemma 11 by considering $\mathsf{x} \subseteq DE$ in every of them, to obtain that $\mathcal{C}_P \cap D_{\mathsf{x}}$ is empty. Hence, we have that D_{b} and D_{x} are disjoint. □

Proof of 1-Chord lemma (Lemma 2). Using Lemma 12, we can ensure that P_n contains a disk $\mathcal{C}$ tangent to three consecutive sides, say the sides s_{i-1}, s_i, and s_{i+1} for some $i \in \{0, 1, \ldots, n-1\}$, such that: the lines $\ell(s_{i-1})$ and $\ell(s_{i+1})$ are not parallel, and their intersection point and the interior of $\mathcal{C}$ belong to different halfplanes bounded by the line $\ell(s_i)$. The bisector of s_{i-1} and s_{i+1} will cross the interior of at most one side s_j of the set $S = \{s_0, s_1, \ldots, s_{n-1}\} \setminus \{s_{i-1}, s_i, s_{i+1}\}$. For any other side $s_k \in S \setminus \{s_j\}$ we have $D_i \cap D_k = \emptyset$, by Lemma 13. The lemma thus follows. □

4 Part II: Proof of No-3-Cycles lemma (Lemma 3)

Lemma 14. *Let $ABCD$ be a convex quadrilateral with vertices A, B, C, and D, so that the lines $\ell(B, C)$ and $\ell(A, D)$ intersect at the point P, and the line $\ell(A, B)$ separates P and the interior of $ABCD$ (see Figure 11(left)). The disk $\mathcal{C}$ with center O is contained in $ABCD$ and tangent to the sides AB, BC, and DA, the line $\ell(A, O)$ intersects the side BC, and the line $\ell(B, O)$ intersects the side DA. Then, the disks D_{AB} and D_{CD} are disjoint.*

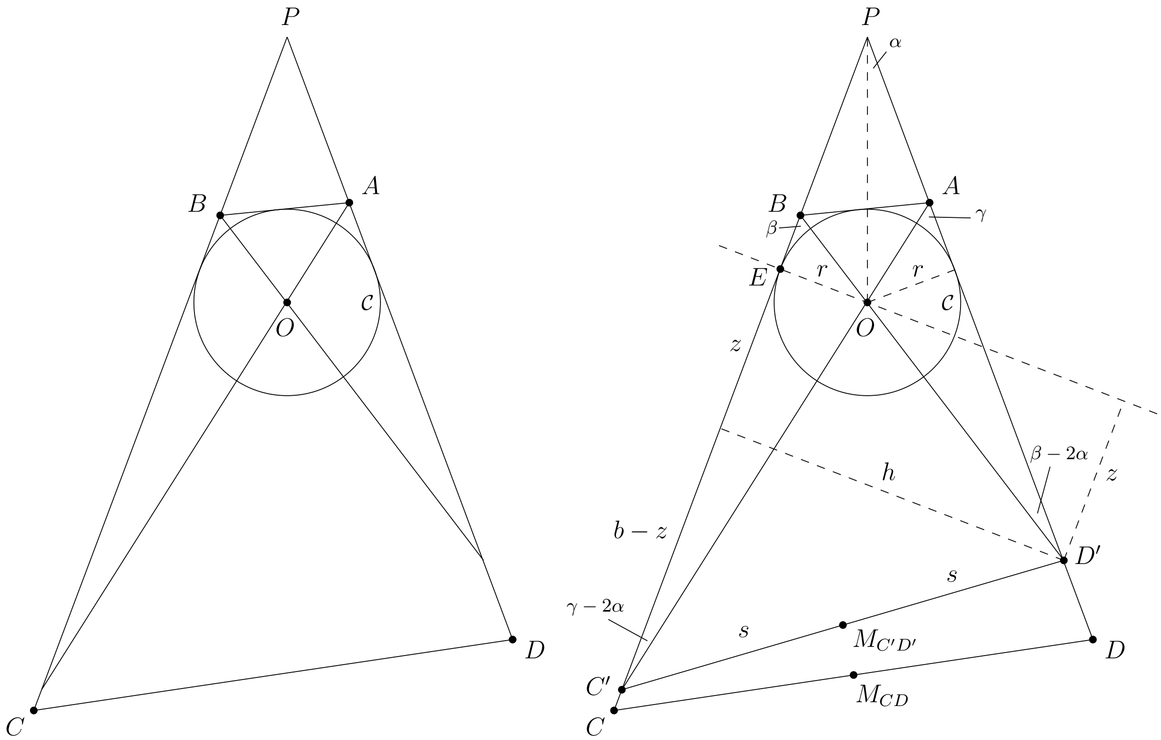

Figure 11: Illustration (left) and proof (right) of Lemma 14.

Proof. (Refer to Figure 14(right) throughout the proof) Let E be the point of tangency between $\mathcal{C}$ and BC, and $C' = \ell(A, O) \cap BC$, and $D' = \ell(B, O) \cap DA$. Let r be the radius of $\mathcal{C}$, $b = |C'E|$, $z = dist(D', \ell(E, O))$, $h = dist(D', \ell(P, C))$, $s = |C'D'|/2$, $\alpha = \angle OPA = \angle OPB$, $\beta = \angle OBA = \angle OBC$, and $\gamma = \angle OAD = \angle OAB$. Assume w.l.o.g. that $\beta \geq \gamma$. Observe that $\gamma > 2\alpha$ since $\ell(A, O)$ intersects BC. Analogously, $\beta > 2\alpha$ since $\ell(B, O)$ intersects DA. Note also that $\pi + 2\alpha = 2\beta + 2\gamma$.

The disk $\mathcal{C}_P$ with center P and radius $|PE|$ contains D_{AB}, by Lemma 7. Then, it suffices to prove that $\mathcal{C}_P$ and D_{CD} are disjoint, which follows by proving that $\mathcal{C}_P$ and $D_{C'D'}$ are disjoint. The reason of this last statement is that any point Q of D_{CD} in the triangle ΔPCD also belongs to $D_{C'D'}$. Indeed, $Q \in D_{CD} \cap \Delta PCD$ implies that $\angle CQD \geq \pi/2$ by Thales' theorem, and we also have $\angle C'QD' > \angle CQD$. Then, Q also belongs to $D_{C'D'}$ by Thales' theorem. We will prove in the following that $\ell(E, O)$ separates the interior of $\mathcal{C}_P$ from the whole $D_{C'D'}$.

We need to prove that the radius s of $D_{C'D'}$ is less than the distance $dist(M_{C'D'}, \ell(E, O)) = (b+z)/2$, where $M_{C'D'}$ denotes the midpoint of $C'D'$. That is, we need to show that $(b+z)^2 > (2s)^2$, where $(2s)^2 = h^2 + (b-z)^2$. This is equivalent to proving that $4bz > h^2$, with

$$b \;=\; r \cdot \cot(\gamma - 2\alpha) \;=\; r \cdot \cot(\pi/2 + \alpha - \beta - 2\alpha)) \;=\; r \cdot \tan(\beta + \alpha),$$

$$z \;=\; |D'O| \cdot \cos\beta \;=\; \left(\frac{r}{\sin(\beta - 2\alpha)}\right) \cos\beta,$$

and

$$h \;=\; r + |D'O| \cdot \sin\beta \;=\; r + \left(\frac{r}{\sin(\beta - 2\alpha)}\right) \sin\beta.$$

This is equivalent to verifying

$$4 \cdot \frac{\tan(\beta+\alpha)\cos\beta}{\sin(\beta-2\alpha)} \;>\; \left(1+\frac{\sin\beta}{\sin(\beta-2\alpha)}\right)^2.$$

Since $2\alpha < \beta$ we have $\sin(\beta-2\alpha) > 0$. On the other hand, given that $\pi + 2\alpha = 2\beta + 2\gamma$ and $\gamma > 2\alpha$, we have $\beta+\alpha < \beta+\gamma-\alpha = \pi/2$, and then $\cos(\beta+\alpha) > 0$. Hence, the above inequation is equivalent to

$$4 \cdot \sin(\beta+\alpha)\sin(\beta-2\alpha)\cos\beta \;>\; (\sin(\beta-2\alpha)+\sin\beta)^2\cos(\beta+\alpha). \tag{1}$$

Since the sine function is concave in $[0,\pi/2]$, for all $x, y \in [0,\pi/2]$ we have

$$\frac{\sin x + \sin y}{2} \;\leq\; \sin\left(\frac{x+y}{2}\right),$$

by Jensen's innequality, and then

$$(\sin(\beta-2\alpha)+\sin\beta)^2 \;\leq\; \left(2\cdot\sin\left(\frac{\beta-2\alpha+\beta}{2}\right)\right)^2 \;=\; 4\cdot\sin^2(\beta-\alpha).$$

Hence, we have

$$4\cdot\sin^2(\beta-\alpha)\cos(\beta+\alpha) \;\geq\; (\sin(\beta-2\alpha)+\sin\beta)^2\cos(\beta+\alpha).$$

and then to prove inequation (1) it suffices to prove

$$\sin(\beta+\alpha)\sin(\beta-2\alpha)\cos\beta \;>\; \sin^2(\beta-\alpha)\cos(\beta+\alpha). \tag{2}$$

Note that

$$\begin{aligned}
& \sin(\beta+\alpha)\sin(\beta-2\alpha)\cos\beta \\
= \;& (\sin\beta\cos\alpha+\cos\beta\sin\alpha)(\sin\beta\cos2\alpha-\cos\beta\sin2\alpha)\cos\beta \\
= \;& (\sin\beta\cos\alpha+\cos\beta\sin\alpha)(\sin\beta\cos^2\alpha-\sin\beta\sin^2\alpha-2\cos\beta\sin\alpha\cos\alpha)\cos\beta \\
= \;& \sin^2\beta\cos\beta\cos^3\alpha-\sin^2\beta\cos\beta\sin^2\alpha\cos\alpha-2\sin\beta\cos^2\beta\sin\alpha\cos^2\alpha \\
& +\sin\beta\cos^2\beta\sin\alpha\cos^2\alpha-\sin\beta\cos^2\beta\sin^3\alpha-2\cos^3\beta\sin^2\alpha\cos\alpha,
\end{aligned}$$

and

$$\begin{aligned}
& \sin^2(\beta-\alpha)\cos(\beta+\alpha) \\
= \;& (\sin\beta\cos\alpha-\cos\beta\sin\alpha)^2(\cos\beta\cos\alpha-\sin\beta\sin\alpha) \\
= \;& (\sin^2\beta\cos^2\alpha+\cos^2\beta\sin^2\alpha-2\sin\beta\cos\beta\sin\alpha\cos\alpha)(\cos\beta\cos\alpha-\sin\beta\sin\alpha) \\
= \;& \sin^2\beta\cos\beta\cos^3\alpha+\cos^3\beta\sin^2\alpha\cos\alpha-2\sin\beta\cos^2\beta\sin\alpha\cos^2\alpha \\
& -\sin^3\beta\sin\alpha\cos^2\alpha-\sin\beta\cos^2\beta\sin^3\alpha+2\sin^2\beta\cos\beta\sin^2\alpha\cos\alpha.
\end{aligned}$$

Then, subtracting the above equations, we have

$$\sin(\beta+\alpha)\sin(\beta-2\alpha)\cos\beta-\sin^2(\beta-\alpha)\cos(\beta+\alpha)$$

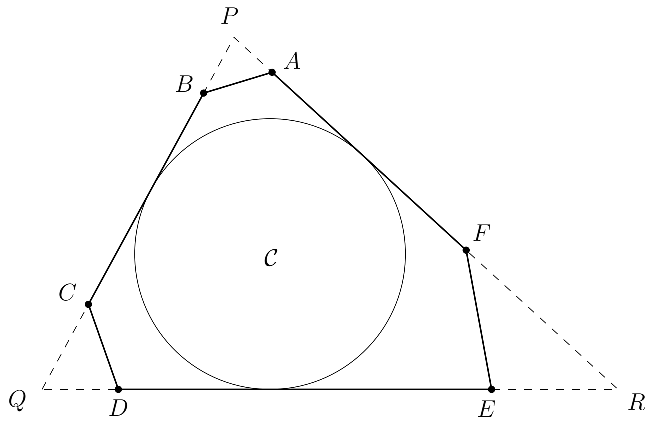

Figure 12: Proof of Lemma 15.

$$
\begin{aligned}
&= -3\cos^3\beta\sin^2\alpha\cos\alpha - 3\sin^2\beta\cos\beta\sin^2\alpha\cos\alpha + \sin^3\beta\sin\alpha\cos^2\alpha \\
&\quad + \sin\beta\cos^2\beta\sin\alpha\cos^2\alpha \\
&= \sin\alpha\cos\alpha\left(-3\cos\beta\sin\alpha(\cos^2\beta+\sin^2\beta) + \sin\beta\cos\alpha(\cos^2\beta+\sin^2\beta)\right) \\
&= \sin\alpha\cos\alpha\left(-3\cos\beta\sin\alpha + \sin\beta\cos\alpha\right).
\end{aligned}
$$

To prove inequation (2), it suffices to show that

$$-3\cos\beta\sin\alpha + \sin\beta\cos\alpha \;>\; 0,$$

that is, $\tan\beta > 3\cdot\tan\alpha$. Given that $\pi + 2\alpha = 2\beta + 2\gamma > 8\alpha$, we have $\alpha < \pi/6$. Furthermore, $\pi + 2\alpha = 2\beta + 2\gamma \leq 4\beta$ implies $\beta \geq \pi/4 + \alpha/2$. Then, note that

$$
\begin{aligned}
\tan\beta \;&\geq\; \tan(\pi/4+\alpha/2) \;=\; \frac{\sin(\pi/4+\alpha/2)}{\cos(\pi/4+\alpha/2)} \;=\; \frac{\cos(\alpha/2)+\sin(\alpha/2)}{\cos(\alpha/2)-\sin(\alpha/2)} \\
&=\; \frac{(\cos(\alpha/2)+\sin(\alpha/2))^2}{\cos^2(\alpha/2)-\sin^2(\alpha/2)} \;=\; \frac{1+\sin\alpha}{\cos\alpha} \;>\; 3\cdot\frac{\sin\alpha}{\cos\alpha} \;=\; 3\cdot\tan\alpha,
\end{aligned}
$$

because $\sin\alpha < \sin(\pi/6) = 1/2$ given that $0 < \alpha < \pi/6$. $\square$

Lemma 15. *Let P, Q, R, A, B, C, D, E, and F be points defining the triangle ΔPQR, and the convex hexagon $ABCDEF$ inscribed in PQR in the following manner: the points B and C are in PQ, the points D and E are in QR, the points F and A are in RP, and $ABCDEF$ contains the disk $\mathcal{C}$ incribed to PQR in its interior. Furthermore, $\mathcal{C}$ is tangent to BC, DE, and FA (see Figure 12). Then, at least one of the following statements is satisfied:*

(a) D_{AB} and D_{DE} are disjoint.

(b) D_{CD} and D_{FA} are disjoint.

(c) D_{EF} and D_{BC} are disjoint.

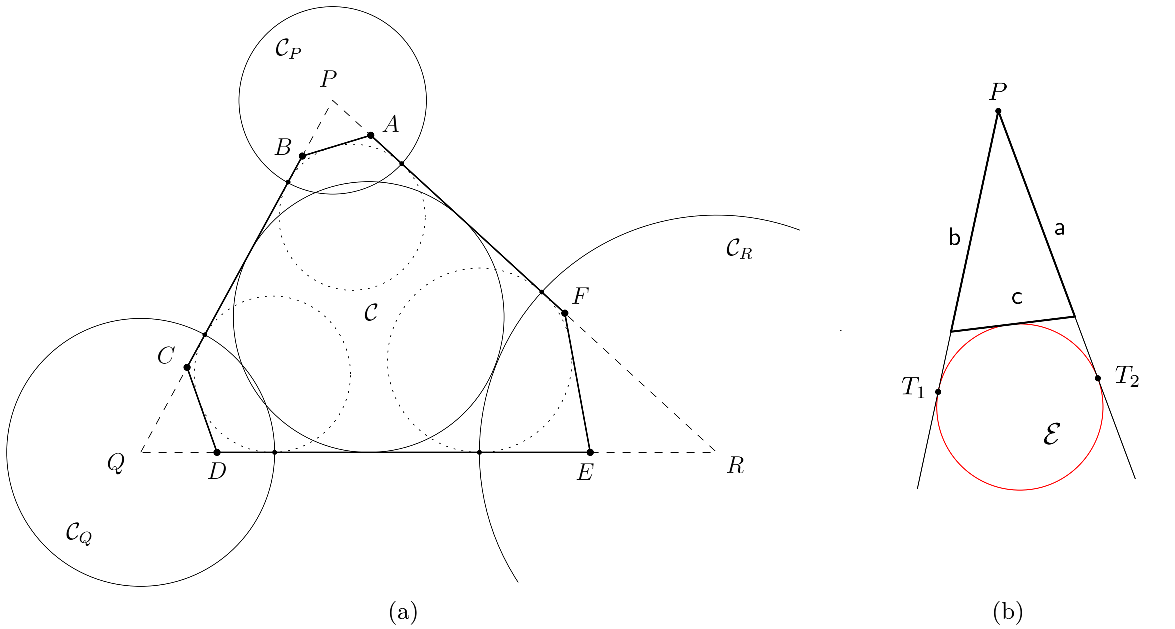

Figure 13: (a) Proof of Lemma 15. (b) Since $\mathcal{E}$ is the excircle of the triangle with sides a, b, and c, tangent to c, and to the lines $\ell(\mathsf{a})$ and $\ell(\mathsf{b})$, then $|PT_1| = |PT_2| = (1/2)(|\mathsf{a}| + |\mathsf{b}| + |\mathsf{c}|)$.

Proof. For $t \geq 0$, let $B(t), C(t) \in BC$, $D(t), E(t) \in DE$, and $F(t), A(t) \in FA$ be the six points such that $|AA(t)| = |BB(t)| = |CC(t)| = |DD(t)| = |EE(t)| = |FF(t)| = t$, and the hexagon $A(t)B(t)C(t)D(t)E(t)F(t)$ is convex and satisfies the same conditions as $ABCDEF$. Let t^* denote the maximum possible value of t. Let $\mathcal{E}_P(t)$ be the disk whose boundary is the excircle of the triangle $\Delta PB(t)A(t)$ that is contained in ΔPQR. Let $\mathcal{C}_P(t)$ denote the disk with center P and radius $|PT(t)|$, where $T(t)$ denotes the point of tangency between $\mathcal{E}_P(t)$ and PQ (see Figure 13a for the case $t = 0$). Analogously, we define the disk $\mathcal{C}_Q(t)$ centered at Q, and the disk $\mathcal{C}_R(t)$ centered at R. Since $D_{AB} = D_{A(0)B(0)}$ is contained in $\mathcal{C}_P = \mathcal{C}_P(0)$ (Lemma 7), to prove statement (a) it suffices to prove that $\mathcal{C}_P$ and $D_{DE} = D_{D(0)E(0)}$ are disjoint, which is equivalent to proving that

$$|PM_{DE}| \; > \; |PT| + \frac{|DE|}{2}, \tag{3}$$

where $T = T(0)$, $M_{D(t)E(t)}$ is the midpoint of $D(t)E(t)$, and $M_{DE} = M_{D(0)E(0)}$. For every $t \in [0, t^*]$, observe that $|PM_{D(t)E(t)}| = |PM_{D(0)E(0)}| = |PM_{DE}|$ since $M_{D(t)E(t)} = M_{D(0)E(0)} = M_{DE}$. Furthermore, $|D(t)E(t)| = |D(0)E(0)| - 2t = |DE| - 2t$.

We use now the following known claim regarding a triangle and an excircle: Given a triangle with sides a, b, and c, let $\mathcal{E}$ be the excircle of the triangle tangent to c, then also tangent to the lines $\ell(\mathsf{a})$ and $\ell(\mathsf{b})$, respectively. Then, the segment with endpoints the common vertex of a and b and the tangency point between $\mathcal{E}$ and $\ell(\mathsf{a})$ (resp. $\ell(\mathsf{b})$) has length $(1/2)(|\mathsf{a}| + |\mathsf{b}| + |\mathsf{c}|)$ (see Figure 13b).

By the above claim, since $\mathcal{E}_P(t)$ is an excircle of $\Delta PA(t)B(t)$, we also have

$$\begin{aligned}
|PT(t)| &= \frac{1}{2}\left(|PB(t)| + |B(t)A(t)| + |A(t)P|\right) \\
&= \frac{1}{2}\left(|PB(0)| + t + |B(t)A(t)| + |A(0)P| + t\right)
\end{aligned}$$

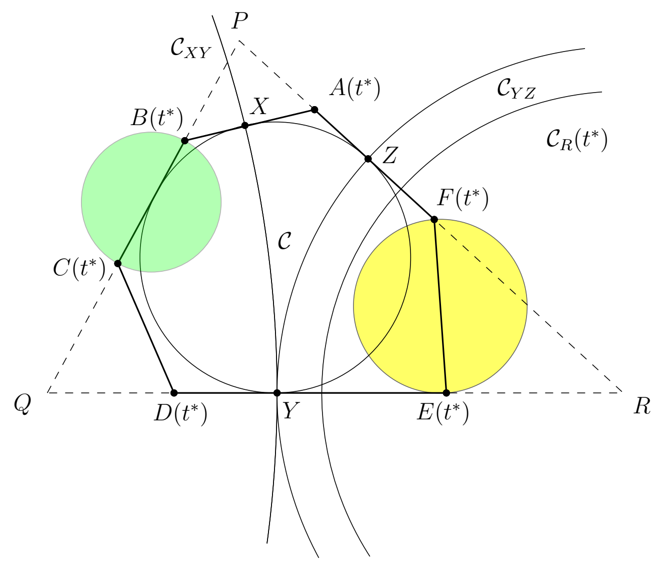

Figure 14: Proof of Lemma 15.

$$= \frac{1}{2}(|PB| + |B(t)A(t)| + |AP|) + t.$$

Consider the function $G : [0, t^*] \to \mathbb{R}$ defined as follows:

$$G(t) = |PM_{D(t)E(t)}| - |PT(t)| - \frac{|D(t)E(t)|}{2},$$

which satisfies

$$\begin{aligned} G(t) &= |PM_{D(t)E(t)}| - |PT(t)| - \frac{|D(t)E(t)|}{2} \\ &= |PM_{DE}| - \frac{1}{2}(|PB| + |B(t)A(t)| + |AP|) - t - \frac{|DE|}{2} + t \\ &= |PM_{DE}| - \frac{1}{2}(|PB| + |B(t)A(t)| + |AP|) - \frac{|DE|}{2}. \end{aligned}$$

Since the function $|B(t)A(t)|$ is increasing in the range $t \in [0, t^*]$, we have that

$$|PM_{DE}| - |PT| - \frac{|DE|}{2} = G(0) \geq G(t^*) = |PM_{D(t^*)E(t^*)}| - |PT(t^*)| - \frac{|D(t^*)E(t^*)|}{2}.$$

Then, to prove inequation (3) and then statement (a), it suffices to show that $G(t^*) > 0$, which is equivalent to showing that $\mathcal{C}_P(t^*)$ and $D_{D(t^*)E(t^*)}$ are disjoint. Analogously, to prove statement (b) it suffices to show that $\mathcal{C}_Q(t^*)$ and $D_{F(t^*)A(t^*)}$ are disjoint, and to prove statement (c) it suffices to show that $\mathcal{C}_R(t^*)$ and $D_{B(t^*)C(t^*)}$ are disjoint.

Observe from the defintion of t^* that $\mathcal{C}$ is tangent to at least one of the segments $A(t^*)B(t^*)$, $C(t^*)D(t^*)$, and $E(t^*)F(t^*)$. Assume w.l.o.g. that $\mathcal{C}$ is tangent to $A(t^*)B(t^*)$. Let X, Y, and Z be the points of tangency between $\mathcal{C}$ and the segments $A(t^*)B(t^*)$, $D(t^*)E(t^*)$, and $F(t^*)A(t^*)$, respectively. Further assume w.l.o.g. that the line $\ell(Q, R)$ is horizontal, and either the lines $\ell(A(t^*), B(t^*))$ and $\ell(Q, R)$ are parallel or the point $\ell(A(t^*), B(t^*)) \cap \ell(Q, R)$ is to the left of Q (see Figure 14 in

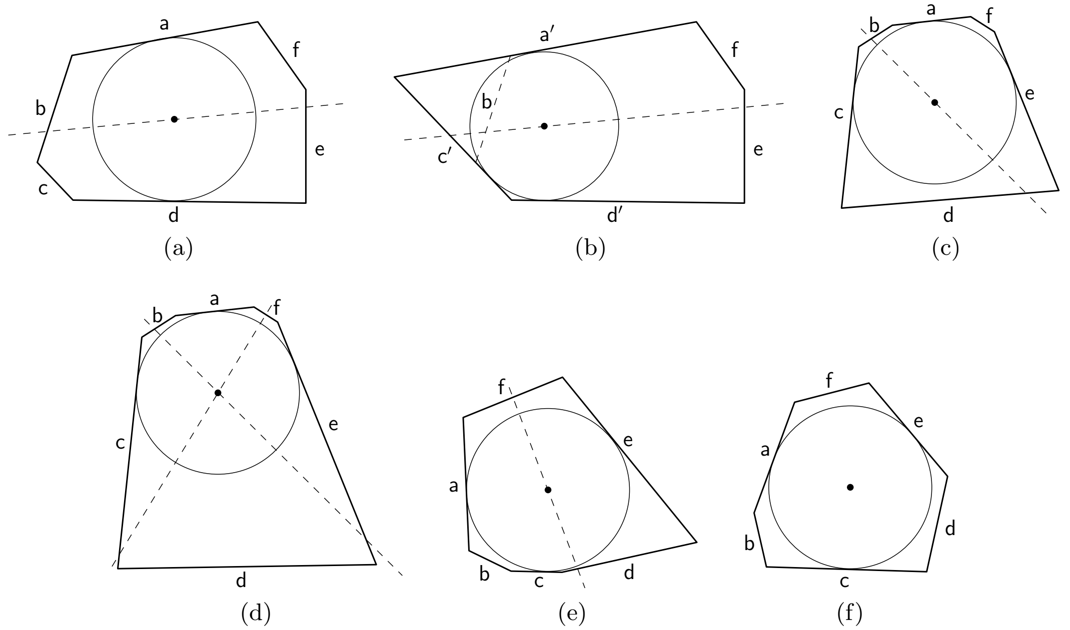

Figure 15: Proof of Lemma 3.

which the latter case occurs). In the former case, let $\mathcal{C}_{XY}$ denote the halfplane with the points in or to the left of the vertical line $\ell(X, Y)$. In the latter case, let $\mathcal{C}_{XY}$ denote the disk centered at $\ell(A(t^*), B(t^*)) \cap \ell(Q, R)$ whose boundary contains X and Y. Let $\mathcal{C}_{YZ}$ denote the disk with center R and radius $|RY| = |RZ|$. By Lemma 7 and construction, we have both

$$D_{B(t^*)C(t^*)} \subset D_{B(t^*)Q} \subset \mathcal{C}_{XY} \quad \text{and} \quad D_{E(t^*)F(t^*)} \subset \mathcal{C}_R(t^*) \subseteq \mathcal{C}_{YZ},$$

which implies that $D_{B(t^*)C(t^*)}$ and $D_{E(t^*)F(t^*)}$ are disjoint. Hence, statement (c) is satisfied and the lemma follows. $\square$

Proof of No-3-Cycles lemma (Lemma 3). By extending a, b, c, d, e, f, we can consider that a, b, c, d, e, f are the sides of an (unbounded) convex 6-gon P_6. The proof is split into several cases. Suppose that there exists a disk contained in P_6 and tangent to two opposed sides, say w.l.o.g. that the disk is tangent to a and d. Further assume w.l.o.g. that d is horizontal, the bisector of a and d intersects the side e, and either the lines $\ell(\mathsf{a})$ and $\ell(\mathsf{d})$ are parallel or the point $\ell(\mathsf{a}) \cap \ell(\mathsf{d})$ is to the left of d (see Figure 15a). Using Lemma 13 with a disk tangent to extensions a', c', and d' of a, c, and d, respectively, it follows that $D_\mathsf{c} \cap D_\mathsf{f} = \emptyset$ (see Figure 15b).

The next cases use similar arguments (i.e. applying Lemma 13). If there does not exist any disk contained in P_6 and tangent to two opposed sides, then there must exist a disk contained in P_6 and tangent to three pairwise non-consecutive sides. Assume w.l.o.g. that such a disk is tangent to a, c, and e. If the lines $\ell(\mathsf{a})$, $\ell(\mathsf{c})$, and $\ell(\mathsf{e})$ do not bound a triangle that contains P_6 (see Figure 15c), then we proceed as follows. Assume w.l.o.g. that either $\ell(\mathsf{c})$ and $\ell(\mathsf{e})$ are parallel or the point $\ell(\mathsf{c}) \cap \ell(\mathsf{e})$ is separated from P_6 by $\ell(\mathsf{a})$, as in Figure 15c. If the bisector of a and c intersects d (see Figure 15c), then $D_\mathsf{b} \cap D_\mathsf{e} = \emptyset$ by Lemma 13. Analogously, if the bisector of a and e intersects d, then $D_\mathsf{c} \cap D_\mathsf{f} = \emptyset$. Suppose now that neither the bisector of a and c intersects d, nor the bisector of

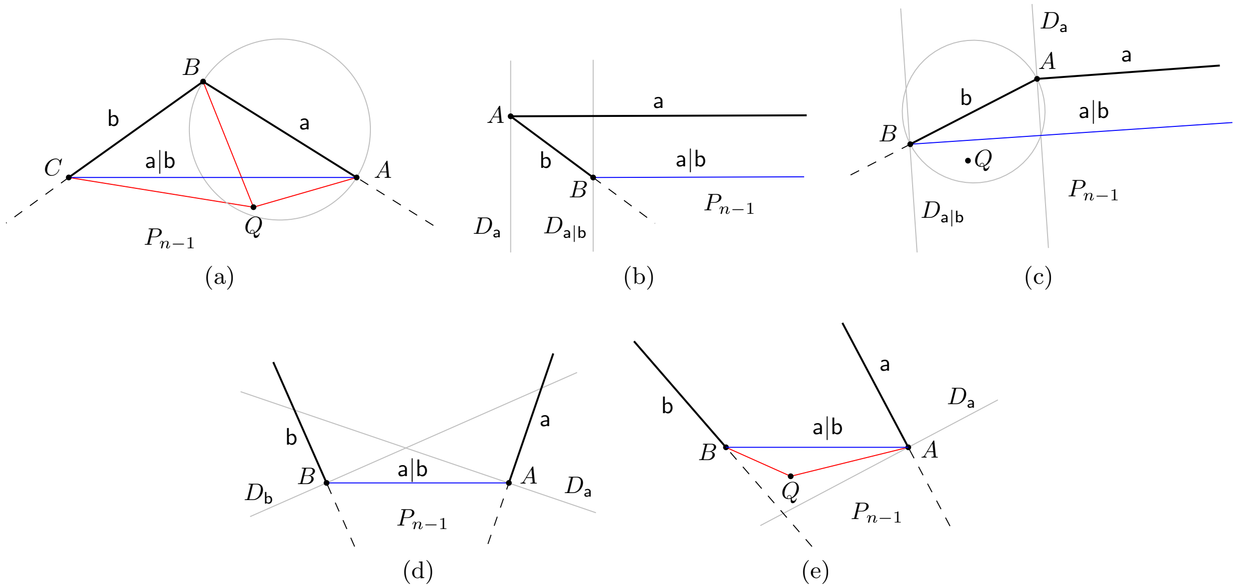

Figure 16: Proof of Lemma 16.

a and e intersects d (see Figure 15d). Then, we have that $D_{\mathsf{a}} \cap D_{\mathsf{d}} = \emptyset$, by Lemma 14. Otherwise, if the lines $\ell(\mathsf{a})$, $\ell(\mathsf{c})$, and $\ell(\mathsf{e})$ do bound a triangle that contains P_6 (see Figure 15e), then we proceed as follows. If the bisector of a and e does not intersect c (see Figure 15e), say w.l.o.g. that it intersects d, then we have $D_{\mathsf{c}} \cap D_{\mathsf{f}} = \emptyset$. Symmetric arguments can be given if the bisector of a and c does not intersect e, or the bisector of c and e does not intersect a. Otherwise, if the bisector of each two sides among a, c, and e intersects the third one (see Figure 15f), then $D_{\mathsf{a}} \cap D_{\mathsf{d}} = \emptyset$, or $D_{\mathsf{b}} \cap D_{\mathsf{e}} = \emptyset$, or $D_{\mathsf{c}} \cap D_{\mathsf{f}} = \emptyset$, by Lemma 15. All the cases are covered, and the lemma follows. ☐

5 Part III: Proof of Main theorem (Theorem 4)

Given an (unbounded) convex polygon and two sides a and b of it, we define the segment (or halfline) $\mathsf{a}|\mathsf{b}$ in the case where a and b are consecutive sides, or both are the two halfline sides of the polygon when it is unbounded, as follows: If a and b are consecutive segments, then $\mathsf{a}|\mathsf{b}$ is the diagonal of the polygon connecting an endpoint of a with an endpoint of b. If a is a halfline and b is a segment, then $\mathsf{a}|\mathsf{b}$ is the halfline contained in the polygon, parallel to a, and with apex the vertex of b not in common with a. If both a and b are halflines because the polygon is unbounded, then $\mathsf{a}|\mathsf{b}$ is the segment (i.e. diagonal) that connects the two endpoints of a and b.

Lemma 16. *Let P_n be an (unbounded) convex n-gon, $n \geq 4$, and a and b two sides of P_n such that the segment (or halfline) $\mathsf{a}|\mathsf{b}$ is defined. Let c be another side of P_n such that D_{c} intersects both D_{a} and D_{b}. Then, D_{c} also intersects $D_{\mathsf{a}|\mathsf{b}}$.*

Proof. Let $R_{\mathsf{a}|\mathsf{b}}$ be the convex region bounded by a, b, and $\mathsf{a}|\mathsf{b}$, and $P_{n-1} = P_n \setminus R_{\mathsf{a}|\mathsf{b}}$ the (possibly unbounded) convex $(n-1)$-gon resulting from removing $R_{\mathsf{a}|\mathsf{b}}$ from P_n. To prove the lemma, it suffices to show the following statement: every point Q in $D_{\mathsf{a}} \cap P_{n-1}$, or $D_{\mathsf{b}} \cap P_{n-1}$, is also in $D_{\mathsf{a}|\mathsf{b}}$.

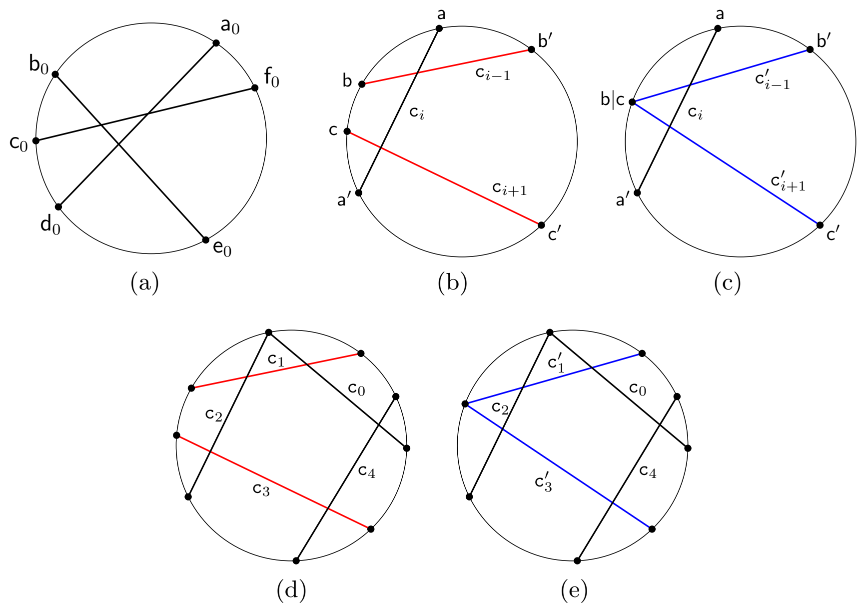

Figure 17: Proof of Theorem 4.

Assume that a and b are segments, so that a has endpoints A and B, b has endpoints B and C, and $\mathsf{a}|\mathsf{b} = AC$. Let Q be a point in $D_\mathsf{a} \cap P_{n-1}$ (see Figure 16a). Then, $\angle AQB \geq \pi/2$ by Thales' theorem. Then, we have $\angle AQC > \angle AQB \geq \pi/2$, which implies that Q is also in $D_{\mathsf{a}|\mathsf{b}}$ by Thales' theorem. Analogulsy, if Q is in $D_\mathsf{b} \cap P_{n-1}$, then it is also in $D_{\mathsf{a}|\mathsf{b}}$. Assume now that a is a halfline and b is a segment, where A is the apex of a, and b has endpoints A and B (see Figure 16b and Figure 16c). In this case, $D_{\mathsf{a}|\mathsf{b}}$ is the halfplane containing a and bounded by the line through B perpendicular to $\mathsf{a}|\mathsf{b}$. If $D_{\mathsf{a}|\mathsf{b}} \subseteq D_\mathsf{a}$ (see Figure 16b), then $P_{n-1} \subset D_{\mathsf{a}|\mathsf{b}}$ and the statement trivially follows. Otherwise, if $D_\mathsf{a} \subset D_{\mathsf{a}|\mathsf{b}}$ (see Figure 16c), then $D_\mathsf{b} \cap P_{n-1} \subset D_{\mathsf{a}|\mathsf{b}}$, and the statement follows. Finally, assume that both a and b are halflines, with A the apex of a, and B the apex of b (see Figure 16d and Figure 16e). If neither D_a contains b nor D_b contains a (see Figure 16d), then the statement trivially follows. Otherwise, assume w.l.o.g. that D_a contains b (see Figure 16e). Let Q be a point in $(D_\mathsf{a} \cup D_\mathsf{b}) \cap P_{n-1}$, and note that $\angle AQB \geq \pi/2$ because the boundary of D_a is perpendicular to a, and a and b are the halflines among the sides of the unbounded P_n. Then, Q belongs to $D_{\mathsf{a}|\mathsf{b}}$ by Thales' theorem, showing that the statement is true. □

Proof of Main theorem (Theorem 4). Let P_n be a convex n-gon with $n \geq 3$. Let $G = (V, E)$ be the intersection graph of the side disks of P_n, and $G_\mathsf{c} = (V_\mathsf{c}, E_\mathsf{c})$ the intersection graph of the chords in the circular embedding of G. If $n = 3, 4$, then G is trivially planar. Thus, assume $n \geq 5$. Suppose that G_c has a 3-length cycle, made of three pairwise intersecting chords, induced by six sides a_0, b_0, c_0, d_0, e_0, f_0 of P_n. Assume w.l.o.g. that these sides appear in this order counter-clockwise along the boundary of P_n (see Figure 17a). Some (or all) of a_0, b_0, c_0, d_0, e_0, f_0 can be extended to obtain the sides $\mathsf{a} \supseteq \mathsf{a}_0$, $\mathsf{b} \supseteq \mathsf{b}_0$, $\mathsf{c} \supseteq \mathsf{c}_0$, $\mathsf{d} \supseteq \mathsf{d}_0$, $\mathsf{e} \supseteq \mathsf{e}_0$, $\mathsf{f} \supseteq \mathsf{f}_0$ of a possibly unbounded convex 6-gon. By Lemma 3, we have that $D_\mathsf{a} \cap D_\mathsf{d} = \emptyset$, $D_\mathsf{b} \cap D_\mathsf{e} = \emptyset$, or $D_\mathsf{c} \cap D_\mathsf{f} = \emptyset$. This implies that $D_{\mathsf{a}_0} \cap D_{\mathsf{d}_0} = \emptyset$, $D_{\mathsf{b}_0} \cap D_{\mathsf{e}_0} = \emptyset$, or $D_{\mathsf{c}_0} \cap D_{\mathsf{f}_0} = \emptyset$. Hence, 3-length cycles do not exist in G_c by contradiction. Let $k \geq 5$ and $c = (\mathsf{c}_0, \mathsf{c}_1, \ldots, \mathsf{c}_{k-1}, \mathsf{c}_0)$ a minimal cycle of length k in G_c, where *minimal* means that no proper subset of $\{\mathsf{c}_0, \mathsf{c}_1, \ldots, \mathsf{c}_{k-1}\}$ form a cycle. Assume that $\mathsf{c}_0, \mathsf{c}_1, \ldots, \mathsf{c}_{k-1}$ are sorted counter-clockwise (as in Figure 17d for $k = 5$), and that they define a set of t endpoints, $k \leq t \leq 2k$. These endpoints correspond to side disks, and then sides, of P_n. Extending some, or all, of such sides we obtain a possibly unbounded convex t-gon P_t. We have two cases: $t > k$ and $t = k$. Suppose that $t > k$. In this case, we can select a chord c_i such that the chords c_{i-1} and c_{i+1} that intersect c_i do not share any endpoint, where subindices are taken modulo k (see Figure 17b). Let a and a' be the sides of P_t that correspond to the endpoints of c_i, let b and b' be the sides that correspond to the endpoints of c_{i-1}, and let c and c' be the sides that correspond to the endpoints of c_{i+1}; so that a, b, c, a' are in this order counter-clockwise along the boundary of P_t. Observe that $\mathsf{b}|\mathsf{c}$ is defined, and let $R_{\mathsf{b}|\mathsf{c}}$ be the convex region bounded by b, c, and $\mathsf{b}|\mathsf{c}$, and let $P_{t-1} = P_t \setminus R_{\mathsf{b}|\mathsf{c}}$. For every chord different from c_{i-1} and c_{i+1} in the cycle c, and sides z and z' of P_{t-1} corresponding to its endpoints, we still have in P_{t-1} that $D_{\mathsf{z}} \cap D_{\mathsf{z}'} \neq \emptyset$. Furthermore, for the sides b' and c', also of P_{t-1},we have both $D_{\mathsf{b}|\mathsf{c}} \cap D_{\mathsf{b}'} \neq \emptyset$ and $D_{\mathsf{b}|\mathsf{c}} \cap D_{\mathsf{c}'} \neq \emptyset$, by Lemma 16. This means that in the intersection graph of the chords in the circular embedding of the side disks of P_{t-1} there exists a cycle of length k, but the chords of the cycle define a set of endpoints of precisely one less element, that is, $t - 1$ endpoints (see the transition from Figure 17d to Figure 17e). Using this transition from P_t to P_{t-1}, we can assume $t = k$ from the beggining and then for every $i \in \{0, 1, \ldots, k-1\}$ we have that c_{i-1} and c_{i+1} share an endpoint. This condition implies that in P_t every side disk defines at least two chords, which contradicts Lemma 2. Hence, the graph G_{c} is bipartite since it cannot contain cycles of odd length, which implies that G is planar by Theorem 1. $\square$

6 Conclusions

We have proved that given any convex n-gon, when drawing for each side a disk having the midpoint of the side as center and the length of the side as diameter, the resulting intersection graph of the n disks is planar. According to the number of edges, the least number of edges is n and it appears, for example, when the n-gon is regular. On the other hand, the number of edges is at most $3n - 6$ and an n-gon, similar to the 6-gon of Figure 2b with 2 big sides and $n - 2$ small ones, has precisely such a number of edges. Finally, we would like to mention that the chromatic number is at most 4 since the graph is planar, and in some cases it equals 4 (e.g., in Figure 2b the disks D_{s_0}, D_{s_2}, D_{s_3}, and D_{s_5} induce the complete graph K_4).

We leave open to study other combinatorial questions under this class of intersection graphs, as done recently by Herrera and Pérez-Lantero [6]. They proved that the treewidth is at most 3, by showing an $O(n)$-time algorithm that builds a tree decomposition of width at most 3, given the polygon as input. This implies that one can construct the intersection graph of the side disks in $O(n)$ time. They further studied the independence number, which is the maximum number of pairwise disjoint disks. The planarity condition implies that for every convex n-gon one can select at least $\lceil n/4 \rceil$ pairwise disjoint disks, and they proved that for every $n \geq 3$ there exist convex n-gons in which one cannot select more than this number. Finally, they showed that this class of intersection graphs includes all outerplanar Hamiltonian graphs except the cycle of length four, and that it is a proper subclass of the planar Hamiltonian graphs.

Acknowledgements

We wish to thank Oswin Aichholzer, Ruy Fabila-Monroy, Thomas Hackl, Tillmann Miltzow, Christian Rubio, Eulàlia Tramuns, Birgit Vogtenhuber, and Frank Duque for inspiring discussions on this topic. We also wish to thank the `GeoGebra` open source software and its developers [7]. First co-author was supported by projects MTM2015-63791-R (MINECO/FEDER) and DGR 2017SGR1336. Second co-author was partially supported by projects CONICYT FONDECYT/Regular 1160543 (Chile), DICYT 041933PL Vicerrectoría de Investigación, Desarrollo e Innovación USACH (Chile), and Programa Regional STICAMSUD 19-STIC-02.

References

[1] S. Cabello and M. Jejčič. Refining the hierarchies of classes of geometric intersection graphs. *Electronic Notes in Discrete Mathematics*, 54:223–228, 2016.

[2] J. H. Conway, H. T. Croft, P. Erdős, and M. J. T. Guy. On the distribution of values of angles determined by coplanar points. *J. London Math. Soc.(2)*, 19(1):137–143, 1979.

[3] L. Danzer. Zur Lösung des Gallaischen Problems über Kreisscheiben in der euklidischen Ebene. *Stud. Sci. Math. Hungar.*, 21:111–134, 1986.

[4] R. Fabila-Monroy, C. Huemer, and E. Tramuns. Note on the number of obtuse angles in point sets. *International Journal of Computational Geometry & Applications*, 24(03):177–181, 2014.

[5] M. Hajja. A condition for a circumscriptible quadrilateral to be cyclic. In *Forum Geometricorum*, volume 8, pages 103–106, 2008.

[6] L. H. Herrera and P. Pérez-Lantero. On the intersection graph of the disks with diameters the sides of a convex n-gon. *arXiv preprint arXiv:1805.10847*, 2018.

[7] M. Hohenwarter. GeoGebra: Ein Softwaresystem für dynamische Geometrie und Algebra der Ebene. Master's thesis, Paris Lodron University, Salzburg, Austria, 2002. (In German.).

[8] C. Huemer and P. Pérez-Lantero. On the disks with diameters the sides of a convex 5-gon. In *XVI Spanish Meeting on Computational Geometry, Barcelona, Spain, July 1-3*, pages 108–111, 2015.

[9] C. Hundack and H. Stamm-Wilbrandt. Planar embedding of hamiltonian graphs via efficient bipartation of circle graphs. 1994. University of Bonn.

[10] P. Koebe. Kontaktprobleme der konformen Abbildung. *Ber. Sächs. Akad. Wiss. Leipzig, Math.-Phys. Kl.*, 88:141–164, 1936.

[11] C. Kuratowski. Sur le probleme des courbes gauches en topologie. *Fundamenta Mathematicae*, 15(1):271–283, 1930.

[12] F. P. Preparata. The medial axis of a simple polygon. In *Mathematical Foundations of Computer Science 1977*, volume 53 of *LNCS*, pages 443–450. 1977.

[13] K. Wagner. Über eine Eigenschaft der ebenen Komplexe. *Mathematische Annalen*, 114(1):570–590, 1937.

[14] R. Wenger. Helly-Type Theorems and Geometric Transversals. In *Handbook of Discrete and Comp. Geom., chapter 4*, pages 63–82. CRC Press, 1997.